MATHEMATICAL MODELING AND COMPUTING, Vol. 9, No. 3, pp. 711–718 (2022)

Influence of uniaxial pressures on dynamic dielectric characteristics of $RbHSO_4$

Levitskii R. R.[1], Zachek I. R.[2]

[1] *Institute for Condensed Matter Physics of the National Academy of Sciences of Ukraine, 1 Svientsitskii Str., 79011, Lviv, Ukraine*
[2] *Lviv Polytechnic National University, 12 S. Bandera Str., 79013, Lviv, Ukraine*

(Received 21 December 2021; Revised 6 August 2022; Accepted 7 August 2022)

Within the modified four-sublattice pseudospin model of deformed $RbHSO_4$ ferroelectrics, using the Glauber method and in the mean field approximation we calculate the dynamic dielectric permittivity of a mechanically clamped crystal and explore its dependence on uniaxial pressures in wide temperature and frequency ranges. A satisfactory quantitative agreement with the experimental data is obtained.

Keywords: *ferroelectrics, dielectric permittivity, pressure effects.*
2010 MSC: 82D45 **DOI:** 10.23939/mmc2022.03.711

1. Introduction

Studies of the effects produced by mechanical stresses of different symmetries on the physical characteristics of ferroelectrics give a deeper insight into the mechanisms of the phase transitions in these crystals and also allow one to search for new physical effects, not observed at ambient pressure.

Rubidium hydrosulphate $RbHSO_4$ (RHS) is an order-disorder ferroelectric. It has a single Curie point ($T_c = 265\,\mathrm{K}$) [1]. The spontaneous polarization arises continuously, indicating the second order phase transition. In the high-temperature phase the crystal structure of RHS is monoclinic, the space group $P2_1/c - C_{2h}^5$. Below the transition point the crystal symmetry is still monoclinic, but the space group changes to $Pc - C_s^2$ [1–3]. In both phases the unit cell contains eight molecules: $Z = 8$.

The phase transition is associated with motion of the sulphate groups $(SO_4)_{11}$, $(SO_4)_{12}$, $(SO_4)_{13}$, $(SO_4)_{14}$ between two asymmetric equilibrium positions. The complexes $(SO_4)_{21}$, $(SO_4)_{22}$, $(SO_4)_{23}$, $(SO_4)_{24}$ are fully ordered at all temperatures and do not play any role in the ferroelectric phase transition. These complexes form the lattice of elementary dipoles, directed along the z axis (Fig. 1).

The dipole moments, formed in the paraelectric phase by the (SO_4) complexes of the (14), (12) types are parallel to each other and antiparallel to the dipole moments, formed by the complexes of the (11) and (13) types, respectively. Similarly, the dipole moments, formed by the complexes of the (21) and (22) type are antiparallel to the dipole moments formed by the (23) and (24) complexes.

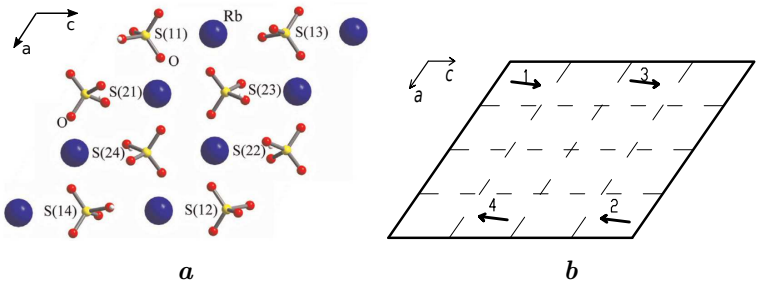

a ***b***

Fig. 1. The primitive cell of $RbHSO_4$ (***a***) and the scheme of the orientation of effective dipole moments $\mathbf{d}_{qf}$ of the sulphate groups $(SO_4)_{1f}$ in the paraelectric phase (***b***).

Two equilibrium positions (potential wells) of these complexes $(1f)$ $(f = 1, 2, 3, 4)$ are not equivalent. Above the transition temperature T_c the complexes $(1f)$ sit in their more energetically favourable equilibrium positions (deeper potential wells). Mathematically the non-equivalence of the equilibrium positions expresses via an additional

longitudinal field Δ, acting on the dipole formed by the sulphate complex. These fields are antiparallel for the (11) and (14) complexes, as well as for the (13) and (12) complexes.

In [4] the four-sublattice model with an asymmetric two-well potential has been proposed for the $RbHSO_4$ crystal, which also takes into account the piezoelectric coupling between the pseudospin and lattice subsystems. This model permitted to obtain a qualitatively correct description of the elastic constants, and a quantitatively correct description of the static and dynamic dielectric and thermal properties of this crystal; in [5] the dielectric properties of deuterated $RbDSO_4$ have been successfully described by the same model. The influence of hydrostatic pressure on the phase transition and longitudinal dielectric permittivity of $RbHSO_4$ were explored [6]; an attempt to predict the effects of the uniaxial pressures and the shear stress σ_5 on the dielectric permittivity was made in [6,7]. However, the model [4] does not take into account the splitting of the parameters of interactions between the pseudospins in presence of the shear strains ε_4 or ε_6; hence, no reliable prediction of the shear stresses σ_4 or σ_6 effects on the thermodynamic characteristics can be made within its framework.

In [8] the model [4] of the $RbHSO_4$ crystal has been modified to the cases, when the system symmetry is lowered down by the shear stresses σ_4 and σ_6. Influence of these mechanical stresses of different symmetries on the phase transition, dielectric, piezoelectric, elastic, and thermal characteristics of this crystal have been studied. The influence of electric field on these characteristics and the electrocaloric effect have been explored as well.

In the present paper we calculate the temperature and frequency dependence of the dynamic dielectric permittivity of $RbHSO_4$ and explore its behavior in presence of uniaxial pressures.

2. Four-sublattice deformable model

In order to calculate the thermodynamic characteristics of $RbHSO_4$ we use the model [8] and take into account the presence of four structural units (sulphate complexes $(SO_4)_{11}$, $(SO_4)_{12}$, $(SO_4)_{13}$, $(SO_4)_{14}$) in the primitive cell, which move in double asymmetric potential wells. We ascribe to these units the dipole moments $\mathbf{d}_{qf}$, where q is the primitive cell index; f is the index of the dipole moment within the cell ($f = 1, \ldots, 4$). In the paralectric phase the sum of these moments is equal to zero; their orientations are shown in Fig. 1*b*.

The changes $\Delta\mathbf{d}_{qf}$ are responsible for appearance of spontaneous polarization in the ferroelectric phase.

The pseudospin variables $\frac{\sigma_{q1}}{2}, \ldots, \frac{\sigma_{q4}}{2}$ describe reordering of the dipole moments associated with the structure elements $\mathbf{d}_{qf} = \mu_f \frac{\sigma_{qf}}{2}$. The mean values of $\langle\frac{\sigma}{2}\rangle = \frac{1}{2}(n_a - n_6)$ are connected to the differences in the populations of two possible equilibrium positions of groups $(SO_4)_{1f}$: n_a and n_b.

The model Hamiltonian in the pseudospin representation reads

$$\hat{H} = NU_{seed} - \frac{1}{2}\sum_{q,q'}\sum_{f,f'=1}^{4} J_{ff'}(qq')\frac{\sigma_{qf}}{2}\frac{\sigma_{q'f'}}{2} - \sum_{q}\sum_{f=1}^{4}(\Delta_f + \boldsymbol{\mu}_f \boldsymbol{E})\frac{\sigma_{qf}}{2}, \tag{1}$$

where N is the number of the primitive cells.

The term U_{seed} in (1) is the seed energy, which corresponds to the lattice of heavy ions and is not explicitly dependent on the configuration of the pseudospin subsystem. It includes the elastic, piezoelectric, and dielectric parts, expressed via the electric fields E_i ($i = 1, 2, 3$) and strains u_j ($j = 1, \ldots, 6$) [8]:

$$U_{seed} = v\left(\frac{1}{2}\sum_{j,j'=1}^{6} c^0_{jj'}(T)u_j u_{j'} - \sum_{i=1}^{3}\sum_{j=1}^{6} e^0_{ij}u_j E_i - \sum_{i,i'=1}^{3}\frac{1}{2}\chi^{u0}_{ii'}E_i E_{i'}\right). \tag{2}$$

The parameters $c^0_{jj'}(T)$, e^0_{ij}, χ^{u0}_{ij} are the so-called seed elastic constants, coefficients of piezoelectric voltage, and dielectric susceptibilities; v is the primitive cell volume.

The second term (1) describes the interactions between the pseudospins; σ_{qf} is the z-component of the operator of the pseudospin, situated in the q-th cell at the sulphate group $(SO_4)_{1f}$ $(f = 1, 2, 3, 4)$. We write the second term in (1) in the mean field approximation

$$-\frac{1}{2}\sum_{q,q'}\sum_{f,f'=1}^{4} J_{ff'}(qq')\frac{\sigma_{qf}}{2}\frac{\sigma_{q'f'}}{2} = \frac{1}{2}\sum_{\substack{q,q'\\f,f'}} J_{ff'}(qq')\frac{\eta_f}{2}\frac{\eta_{f'}}{2} - \sum_{\substack{q,q'\\f,f'}} J_{ff'}(qq')\frac{\eta_{f'}}{2}\frac{\sigma_{qf}}{2}. \tag{3}$$

The third term in (1) describes the interaction of the pseudospins with the external electric field $\boldsymbol{E}$ and with the local fields Δ_f. The parameters $\boldsymbol{\mu}_f$ are the effective dipole moments per one pseudospin $\boldsymbol{\mu}_1 = \boldsymbol{\mu}_2 = (\mu^x, \mu^y, \mu^z)$, $\boldsymbol{\mu}_3 = \boldsymbol{\mu}_4 = (\mu^x, -\mu^y, \mu^z)$.

The Fourier-transforms of the interaction constants $J_{ff'} = \sum_{q'} J_{ff'}(qq')$ at $\mathbf{k} = 0$ and the local fields Δ_f are linearly expanded over the strains u_j

$$J_{ff'} = J^0_{ff'} + \sum_j \psi_{ff'j}u_j, \quad \Delta_f = \Delta^0_f + \sum_j \varphi_{fj}u_j. \tag{4}$$

With taking into account the crystal symmetry the parameters $J_{ff'}$ read

$$J_{\frac{11}{22}} = J^0_{11} + \sum_{l=1,2,3,5} \psi_{11l}u_l + \psi_{114}u_4 + \psi_{116}u_6, \quad J_{\frac{33}{44}} = J^0_{11} + \sum_l \psi_{11l}u_l - \psi_{114}u_4 - \psi_{116}u_6, \tag{5}$$

$$J_{\frac{12}{34}} = J^0_{12} + \sum_l \psi_{12l}u_l \pm \psi_{124}u_4 \pm \psi_{126}u_6, \qquad J_{\frac{13}{24}} = J^0_{13} + \sum_l \psi_{13l}u_l, \qquad J_{\frac{14}{23}} = J^0_{14} + \sum_l \psi_{14l}u_l,$$

$$\Delta_{\frac{1}{3}} = \Delta^0_1 + \sum_l \varphi_{1l}u_l \pm \varphi_{14}u_4 \pm \varphi_{16}u_6, \qquad \Delta_{\frac{2}{4}} = -\Delta^0_1 - \sum_l \varphi_{1l}u_l \mp \varphi_{14}u_4 \mp \varphi_{16}u_6,$$

As a result, in the mean field approximation the initial Hamiltonian (1) is

$$\hat{H} = NU_{seed} + \frac{N}{8}\sum_{ff'} J_{ff'}\eta_f\eta_{f'} - \sum_q\sum_{f=1}^{4} \mathcal{H}_f\frac{\sigma_{qf}}{2}, \tag{6}$$

where

$$\mathcal{H}_f = \frac{1}{2}\sum_{f'} J_{ff'}\eta_{f'} + \Delta_f + \boldsymbol{\mu}_f\boldsymbol{E}. \tag{7}$$

3. Thermodynamic characteristics of $RbHSO_4$

To calculate the thermodynamic characteristics of $RbHSO_4$ we use the thermodynamic potential per unit cell, obtained in [8] within the mean field approximation

$$g = \frac{G}{N} = U_{seed} + \frac{1}{8}\sum_{f,f'} J_{ff'}\eta_f\eta_{f'} - 4\frac{1}{\beta}\ln 2 - \frac{1}{\beta}\sum_{f=1}^{4}\ln\cosh\frac{\beta}{2}\mathcal{H}_f - v\sum_{j=1}^{6}\sigma_j u_j. \tag{8}$$

From the conditions of the thermodynamic equilibrium

$$\left(\frac{\partial g}{\partial \eta_f}\right)_{E_i,\sigma_i} = 0, \quad \left(\frac{\partial g}{\partial u_j}\right)_{E_i,\sigma_i} = 0$$

we obtain the system of equations for the order parameters η_f and strains u_j:

$$\eta_f = \tanh\frac{\beta}{2}\mathcal{H}_f, \tag{9}$$

$$\sigma_j = \sum_{j'=1}^{6} c^0_{jj'}(T)u_{j'} - \sum_{i=1}^{3} e^0_{ij}E_i - \sum_{f,f'=1}^{4}\frac{\psi_{ff'j}}{8v}\eta_f\eta_{f'} - \sum_{f=1}^{4}\frac{\varphi_{fj}}{2v}\eta_f. \tag{10}$$

For the uniaxial pressure applied along the OX axis $-p_1 \neq 0$, $-p_2 = 0$, $-p_3 = 0$, $\sigma_j = 0$, along the OY axis $-p_2 \neq 0$, $-p_1 = 0$, $-p_3 = 0$, $\sigma_j = 0$, and along the OZ axis $-p_3 \neq 0$, $-p_1 = 0$, $-p_2 = 0$, $\sigma_j = 0$.

4. Dynamic dielectric properties of mechanically clamped $RbHSO_4$ crystal. Analytic results

Hereafter we study the longitudinal dynamic dielectric characteristics, when the shear stresses are absent. In this case the shear strains u_4 and u_6 are equal to zero. We use the approach based on the ideas of the Glauber stochastic model. In this approach the following system of the Glauber equations for the time-dependent one-particle correlation functions of pseudospins is obtained

$$-\alpha\frac{d}{dt}\langle\sigma_{qf}\rangle = \left\langle \sigma_{qf}\left[1-\sigma_{qf}\tanh\frac{1}{2}\beta\varepsilon_{qf}(t)\right]\right\rangle, \tag{11}$$

where the parameter α sets the time scale of the dynamic processes in the system; $\varepsilon_{qf'}(t)$ is the local field acting on the f'th pseudospin in the qth cell; this is the factor at $\sigma_{qf'}/2$ in the initial Hamiltonian.

In the mean field approximation the local fields $\varepsilon_{qf}(t)$ are the factors at $\sigma_{qf}/2$ in the one-particle Hamiltonians (7), reading

$$\varepsilon_{qf} = \mathcal{H}_f = \frac{1}{2}\sum_{f'} J_{ff'}\eta_{f'} + \Delta_f + \boldsymbol{\mu}_f\boldsymbol{E}. \tag{12}$$

As a result, from (11) we obtain the following system of equations for the mean values of pseudospins $\langle\sigma_{qf}\rangle = \eta_f$ within the single-particle approximation

$$\alpha\frac{d}{dt}\eta_f = -\eta_f + \tanh\frac{\beta\mathcal{H}_f}{2}, \tag{13}$$

In solving Eqs. (13) we shall restrict our consideration by the case of small deviations from equilibrium. To this end we present η_f and the effective fields $\mathcal{H}_f$ as sums of the equilibrium parts of the quantities and their fluctuation parts (mechanically clamped crystal), and also expand $\tanh(\ldots)$ in series over $\mathcal{H}_f$, retaining only the zero order and linear terms

$$\eta_f = \tilde{\eta}_f + \eta_{ft}, \tag{14}$$

$$\mathcal{H}_f = \tilde{\mathcal{H}}_f + \mathcal{H}_{ft} = \frac{1}{2}\sum_{f'} J_{ff'}\tilde{\eta}_{f'} + \Delta_f + \mu_f^z E_z + \frac{1}{2}\sum_{f'} J_{ff'}\eta_{f't} + \mu_f^z E_{zt}.$$

$$\tanh\frac{\beta\mathcal{H}_f}{2} = \tanh\frac{\beta\tilde{\mathcal{H}}_f}{2} + K_f\frac{\beta\mathcal{H}_{ft}}{2}, \quad K_f = 1-\tanh^2\frac{\beta\tilde{\mathcal{H}}_f}{2} = 1-\tilde{\eta}_f^2.$$

Substituting (14) into (13) and taking into account Eq. (10), obeyed at equilibrium, we obtain the system of equations for the non-equilibrium contributions to the order parameters

$$\alpha\frac{d}{dt}\eta_{ft} = -\eta_{ft} + K_f\frac{\beta}{2}\left(\frac{1}{2}\sum_{f'} J_{ff'}\eta_{f't} + \mu_f^z E_{zt}\right). \tag{15}$$

In presence of the field E_{zt} from the symmetry considerations it follows that $\eta_{1t} = \eta_{3t}$, $\eta_{2t} = \eta_{4t}$, $\mu_f^z = \mu^z$, and the system of equations (15) reads

$$\frac{d}{dt}\begin{pmatrix}\eta_{1t}\\ \eta_{2t}\end{pmatrix} = \begin{pmatrix}a_{11} & a_{12}\\ a_{21} & a_{22}\end{pmatrix}\begin{pmatrix}\eta_{1t}\\ \eta_{2t}\end{pmatrix} + \begin{pmatrix}b_1\\ b_2\end{pmatrix}\beta\mu^z E_{zt}, \tag{16}$$

where

$$a_{11} = (-1+K_1\frac{\beta}{4}(J_{11}+J_{13}))/\alpha, \qquad a_{12} = K_1\frac{\beta}{4\alpha}(J_{12}+J_{14}), \qquad b_1 = \frac{K_1}{2\alpha}$$

$$a_{21} = K_2\frac{\beta}{4\alpha}(J_{21}+J_{23}), \qquad a_{22} = (-1+K_2\frac{\beta}{4}(J_{22}+J_{24}))/\alpha, \qquad b_2 = \frac{K_2}{2\alpha}. \tag{17}$$

Solving Eqs. (16), we obtain the time-dependent mean values of the pseudospins. The components of the dynamic dielectric susceptibility of a clamped RHS crystal are determined as

$$\chi_{33}(\omega) = \chi_{33}^0 + \lim_{E_{3t}\to 0}\frac{\mu^z}{\upsilon}\frac{d(\eta_{1t}+\eta_{3t})_3}{dE_{3t}}.$$

The obtained susceptibility components consist of the "seed" contribution and two relaxation modes

$$\chi_{33}(\omega) = \chi_{33}^0 + \sum_{l=1}^{2} \frac{\chi l}{1 + i\omega\tau_l}, \tag{18}$$

where

$$\chi_l = \frac{\beta}{v} \frac{\tau_1\tau_2(\mu^z)^2}{\tau_2 - \tau_1}(-1)^{l-1} \left\{b_1 + b_2 + \tau_l[b_1a_{22} + b_2a_{11} - (b_1a_{21} + b_2a_{12})]\right\},$$

$\tau_{1,2}$ are the relaxation times

$$(\tau_{1,2})^{-1} = \frac{1}{2}\left\{-(a_{11} + a_{22}) \pm \sqrt{(a_{11} + a_{22})^2 - 4(a_{12}a_{21} - a_{12}a_{21})}\right\}. \tag{19}$$

The components of the complex dielectric permittivity of the pseudospin subsystem of RHS read

$$\varepsilon'_{33}(\omega) = \varepsilon_{33}^{\varepsilon 0} + \sum_{i=1}^{2} \frac{4\pi\chi_i}{1 + (\omega\tau_i)^2}, \quad \varepsilon''_{33}(\omega) = \sum_{i=1}^{2} \frac{4\pi\omega\tau_i\chi_i}{1 + (\omega\tau_i)^2}. \tag{20}$$

5. Comparison of the numerical calculations with experimental data

The values of the model parameters have been determined in [8] by fitting the calculated characteristics to experimental data for the temperature dependences of the spontaneous polarization $P_3(T)$ [1, 9], dielectric permittivity $\varepsilon_{33}(T)$ in absence of external influence [1,9] and at different values of hydrostatic pressure [10] and electric field [11], molar specific heat $C(T)$ [12], and elastic constants $c_{jj'}(T)$ [13].

The interaction constants in an un-deformed crystal $J^0_{ff'}$ $(f, f' = 1, 2, 3, 4)$ and the local fields Δ^0_f, creating the asymmetry in the populations of two equibrium positions, are the following $J^0_{11}/k_B = J^0_{13}/k_B = 372\,\mathrm{K}$, $J^0_{12}/k_B = J^0_{14}/k_B = 310\,\mathrm{K}$, $\Delta^0_1/k_B = 244.81\,\mathrm{K}$. The rest of the parameters $J^0_{ff'}$ and Δ^0_f are determined by the crystal symmetry, as discussed in (5).

The deformation potentials $\psi_{ff'j}$ and φ_{fj} are: $\tilde\psi_{111} = -1700\,\mathrm{K}$, $\tilde\psi_{112} = -4600\,\mathrm{K}$, $\tilde\psi_{113} = -500\,\mathrm{K}$, $\tilde\psi_{114} = 0\,\mathrm{K}$, $\tilde\psi_{115} = 1200\,\mathrm{K}$, $\tilde\psi_{116} = 3500\,\mathrm{K}$, $\tilde\psi_{121} = -500\,\mathrm{K}$, $\tilde\psi_{122} = -3040\,\mathrm{K}$, $\tilde\psi_{123} = -500\,\mathrm{K}$, $\tilde\psi_{124} = 0\,\mathrm{K}$, $\tilde\psi_{125} = 400\,\mathrm{K}$, $\tilde\psi_{126}/k_B = -7000\,\mathrm{K}$, $\tilde\psi_{ff'j} = \psi_{ff'j}/k_B$. The analysis shows that the calculated thermodynamic characteristics depend on the sums $\psi_{11l} + \psi_{13l}$, $\psi_{12l} + \psi_{14l}$ $(l = 1, 2, 3, 5)$. For the sake of simplicity, we take them to be equal, that is, $\psi_{13l} = \psi_{11l}$, $\psi_{14l} = \psi_{12l}$. The rest of the parameters $\psi_{ff'j}$ are determined by the crystal symmetry of $RbHSO_4$, as discussed in (5), $\varphi_{fj} = 0\,\mathrm{K}$.

The effective dipole moment equals $\mu^z = 2.8 \cdot 10^{-30}\mathrm{C{\cdot}m}$.

The "seed" dielectric susceptibility $\chi^{u0}_{ii'}$, coefficients of piezoelectric voltage e^0_{ij}, and elastic constants c^0_{ij} are: $\chi^{u0}_{33} = 0.159$ (note that in [8] we took it to be equal to 0.35), $\chi^{u0}_{13} = 0.0$; $e^0_{ij} = 0\,\frac{\mathrm{C}}{\mathrm{m}^2}$; $c^0_{11} = 3.06{\cdot}10^{10}\,\frac{\mathrm{H}}{\mathrm{m}^2}$, $c^0_{12} = 1.54{\cdot}10^{10}\,\frac{\mathrm{H}}{\mathrm{m}^2}$, $c^0_{13} = 0.8{\cdot}10^{10}\,\frac{\mathrm{H}}{\mathrm{m}^2}$, $c^0_{22} = 3.8 \cdot 10^{10}\,\frac{\mathrm{H}}{\mathrm{m}^2}$, $c^0_{23} = 0.67 \cdot 10^{10}\,\frac{\mathrm{H}}{\mathrm{m}^2}$, $c^0_{33} = 3.62 \cdot 10^{10}\,\frac{\mathrm{H}}{\mathrm{m}^2}$, $c^0_{44} = 0.48 \cdot 10^{10}\,\frac{\mathrm{H}}{\mathrm{m}^2}$, $c^0_{55} = 0.53 \cdot 10^{10}\,\frac{\mathrm{H}}{\mathrm{m}^2}$, $c^0_{66} = 1.25 \cdot 10^{10}\,\frac{\mathrm{H}}{\mathrm{m}^2}$, $c^0_{15} = c^0_{25} = c^0_{35} = c^0_{46} = 0.0\,\frac{\mathrm{H}}{\mathrm{m}^2}$.

The primitive cell volume of RHS is $v = 0.842 \cdot 10^{-27}\,\mathrm{m}^3$.

The parameter $\alpha = P + R|T - T_c|$, where $P = 1.6 \cdot 10^{-14}\,\mathrm{s}$, $R = -0.011 \cdot 10^{-14}\,\mathrm{s}$.

There are two contributions to the components of the dynamic dielectric permittivity tensor in the $RbHSO_4$ crystal. Only one of these contributions to the permittivities is crucial $(\chi_2 \gg \chi_1)$; the respective relaxation times are $\tau_2 \gg \tau_1$. The magnitude of $(\tau_2)^{-1}$ decreases at approaching the transition temperature and vanishes at $T = T_c$. Influence of the uniaxial pressures p_i on the relaxation time is illustrated in Fig. 2: the

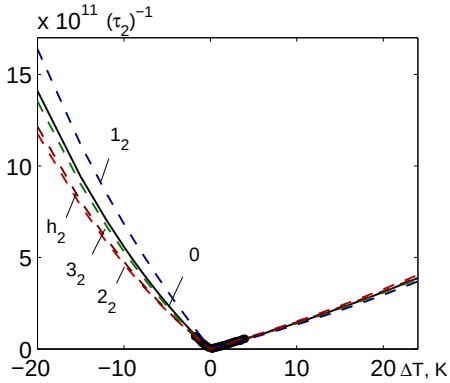

Fig. 2. The temperature dependence of the inverse relaxation time $(\tau_2)^{-1}$ at different values of external pressures. The symbols h_p and 1_p, 2_p, 3_p correspond to the hydrostatic and uniaxial p_1, p_2, p_3 pressures, respectively. The lower index denotes the pressure p (kbar), • [14].

temperature dependences of $(\tau_2)^{-1}$ at different values of pressures are shown. The uniaxial p_2, p_3 and hydrostatic p_h pressures increase the value of the relaxation time τ_2 in the ferroelectric phase at fixed ΔT, whereas the uniaxial pressure p_1 decreases it. In the paraelectric phase the effect of the pressures p_i on the magnitude of the relaxation time τ_2 is much weaker than in the ferroelectric phase; the uniaxial p_2 and hydrostatic p_h pressures decrease τ_2, whereas the p_1, p_3 pressures increase it. The influence of the p_3 pressure on τ_2 is the smallest, as compared to that of the p_1, p_2 pressures.

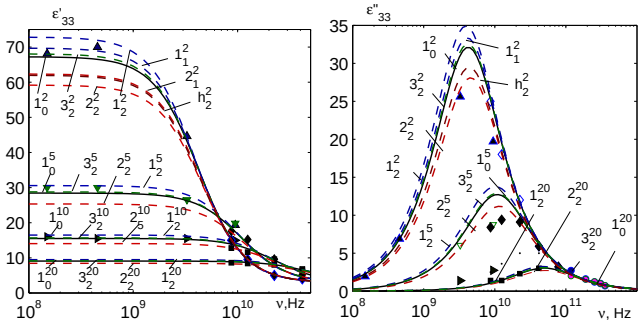

Fig. 3. The frequency dependences of the real ε'_{33} and imaginary ε''_{33} parts of the dielectric permittivity $RbHSO_4$ at different ΔT and different values of the pressures (kbar). The symbols h_p, 1_p, 2_p, 3_p correspond to the hydrostatic and uniaxial p_1, p_2, p_3 pressures, respectively. In the quantities $1_p^{\Delta T}$, $2_p^{\Delta T}$, $3_p^{\Delta T}$, $h_p^{\Delta T}$, $\Delta T = 2.0\,\mathrm{K}$ – $\triangle$ [14], $\Diamond$ [15], $\circ$ [16]; $\Delta T = 5.0\,\mathrm{K}$ – $\triangledown$ [14], $\Diamond$ [15]; $\Delta T = 10.0\,\mathrm{K}$ – $\triangleright$ [14], $\square$ [15]; $\Delta T = 20\,\mathrm{K}$ – $\square$ [15], $\circ$ [16], whereas the lower index denotes the pressure.

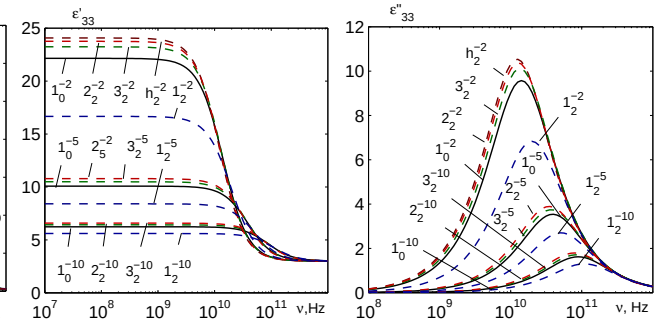

Fig. 4. The frequency dependences of the real ε'_{33} and imaginary ε''_{33} parts of the dielectric permittivity $RbHSO_4$ at different ΔT and different values of the pressures (kbar). The symbols h_p, 1_p, 2_p, 3_p correspond to the hydrostatic and uniaxial p_1, p_2, p_3 pressures, respectively. In the quantities $1_p^{\Delta T}$, $1_p^{\Delta T}$, $1_p^{\Delta T}$, $h_p^{\Delta T}$, $\Delta T = -2.0\,\mathrm{K}$; $\Delta T = -5.0\,\mathrm{K}$; $\Delta T = -10.0\,\mathrm{K}$, whereas the lower index denotes the pressure.

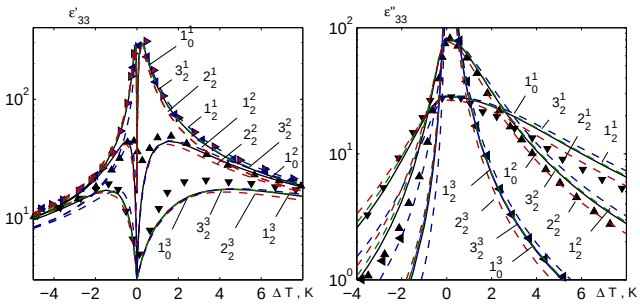

Fig. 5. The temperature dependences of the real ε'_{33} and imaginary ε''_{33} parts of the dielectric permittivity $RbHSO_4$ at different frequencies ν (GHz) and different pressures. The symbols 1_p, 2_p, 3_p correspond to the uniaxial pressures p_1, p_2, p_3, respectively. In the quantities 1_p^i, 2_p^i, 3_p^i the upper index denotes the frequencies: 0.455 – 1, $\blacktriangleleft$ [14]; 3.27 – 2, $\blacktriangle$ [14]; 9.50 – 3, $\blacktriangledown$ [14], whereas the lower index denotes the pressure (kbar).

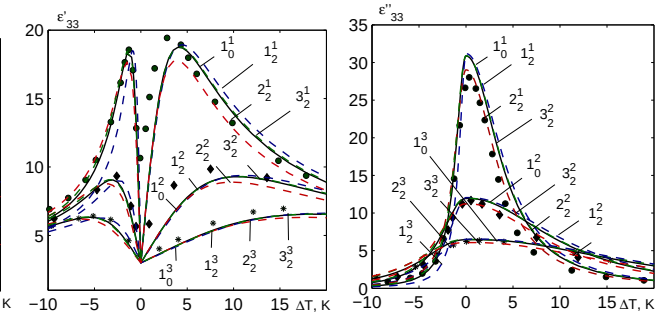

Fig. 6. The temperature dependences of the real ε'_{33} and imaginary ε''_{33} parts of the dielectric permittivity $RbHSO_4$ at different frequencies ν (GHz) and different pressures. The symbols 1_p, 2_p, 3_p correspond to the uniaxial pressures p_1, p_2, p_3, respectively. In the quantities 1_p^i, 2_p^i, 3_p^i the upper index denotes the frequencies: 8.72 – 1, $\bullet$ [17]; 22.55 – 2, $\blacklozenge$ [17]; 41.7 – 3, $*$ [17], whereas the lower index denotes the pressure (kbar).

Related to the relaxation time τ_2^y is the typical for this crystal relaxation frequency $\nu_s = (2\pi\tau_2)^{-1}$, which nominally separates the regions of the low-frequency and high-frequency dynamics of the system.

Since the relaxation time decreases with pressures p_2, p_h in the paraelectric phase, the curves $\varepsilon'_{33}(p_2,\nu)$ and $\varepsilon''_{33}(p_2,\nu)$, $\varepsilon'_{33}(p_h,\nu)$ and $\varepsilon''_{33}(p_h,\nu)$ are shifted downwards by these pressures (Fig. 3), whereas the curves $\varepsilon'_{33}(p_1,\nu)$ and $\varepsilon''_{33}(p_1,\nu)$, $\varepsilon'_{33}(p_3,\nu)$ and $\varepsilon''_{33}(p_3,\nu)$ are shifted upwards, since the relaxation time τ_2 increases with these pressures.

In the ferroelectric phase the increase of the relaxation time τ_2 with the pressures p_2, p_3, p_h leads to the increase of the values of $\varepsilon'_{33}(p,\nu)$ below the dispersion frequency ν_s and to the decrease at $\nu > \nu_s$, whereas the values of $\varepsilon''_{33}(p,\nu)$ are increased by these pressures at all frequencies (Fig. 4).

The pressure p_1 decreases the values of $\varepsilon'_{33}(p_1,\nu)$ at frequencies $\nu < \nu_s$ and increases at $\nu > \nu_s$ (Fig. 4). With increasing $\Delta T = T - T_C$ and frequency, the influence of the pressures p_i on the values of $\varepsilon'_{33}(p_i,\nu)$ and $\varepsilon''_{33}(p_i,\nu)$ weakens.

The dispersion region in the frequency dependences of $\varepsilon'_{33}(p_i,\nu)$ and $\varepsilon''_{33}(p_i,\nu)$ both in the paraelectric and in the ferroelectric phase is shifted to lower frequencies by the pressures p_i (Fig. 3, 4).

Figs. 5, 6, and 7 show the temperature dependences of the real $\varepsilon'_{33}(p_i,T)$ and imaginary $\varepsilon''_{33}(p_i,T)$ parts of the dielectric permittivity of $RbHSO_4$ at the different frequencies ν (low frequencies: Fig. 5, intermediate frequencies: Fig. 6, high frequencies: Fig. 7) and different values of uniaxial pressures p_i.

The influence of uniaxial pressures on the temperature dependences of the dynamic permittivity consists, mainly, of the shifts of the $\varepsilon'_{33}(p_2,T)$ and $\varepsilon''_{33}(p_2,T)$, $\varepsilon'_{33}(p_3,T)$ and $\varepsilon''_{33}(p_3,T)$ curves to higher temperatures due to the increase of the transition temperature T_c with pressures p_2 and p_3, respectively, whereas the curves $\varepsilon'_{33}(p_1,T)$ and $\varepsilon''_{33}(p_1,T)$ shift to lower temperatures.

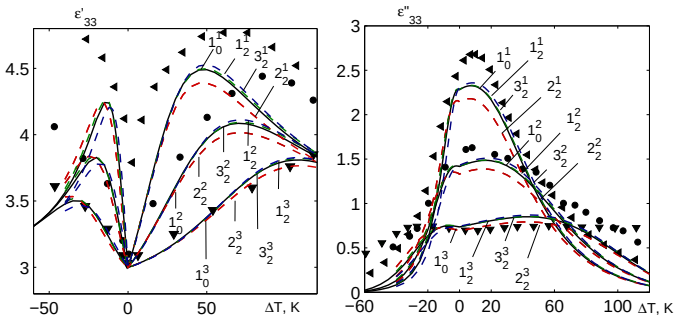

Fig. 7. The temperature dependences of the real ε'_{33} and imaginary ε''_{33} parts of the dielectric permittivity $RbHSO_4$ at different frequencies ν (GHz) and different pressures. The symbols 1_p, 2_p, 3_p correspond to the uniaxial pressures p_1, p_2, p_3, respectively. In the quantities 1^i_p, 2^i_p, 3^i_p the upper index denotes the frequencies: 118 – 1, ◀ [16]; 190 – 2, • [16]; 366 – 3, ▲ [16], whereas the lower index denotes the pressure (kbar).

The permittivity curves $\varepsilon'_{33}(p_1,T)$ and $\varepsilon''_{33}(p_1,T)$ are shifted upwards by the pressure p_1 in the paraelectric phase and downwards in the ferroelectric phase. The values of $\varepsilon'_{33}(p_3,T)$ and $\varepsilon''_{33}(p_3,T)$ are slightly increased by the pressure p_3 in the paraelectric phase. Application of the uniaxial pressure p_2 decreases the magnitudes of $\varepsilon'_{33}(p_2,T)$ and $\varepsilon''_{33}(p_2,T)$ in the paraelectric phase and increases them in the ferroelectric phase.

6. Conclusions

The model of the deformed $RbHSO_4$ crystal predicts a linearly increasing dependence of the transition temperature T_c on the uniaxial pressure p_2, decreasing on the pressure p_1, whereas the pressure p_3 is predicted to hardly affect the transition temperature. Similarly, the influence of p_3 on the dynamic permittivities is minor.

With increasing frequency the influence of the uniaxial pressures p_i on $\varepsilon'_{33}(p_i,T)$ and $\varepsilon'_{33}(p_i,T)$ weakens. The influence of p_i on $\varepsilon'_{33}(p_i,\nu)$ and $\varepsilon''_{33}(p_i,\nu)$ weakens with increasing $\Delta T = T - T_C$.

The obtained temperature and frequency dependences of the dynamic permittivities of $RbHSO_4$ in presence of the uniaxial pressures p_i are the predictions of the model and should be verified experimentally.

[1] Pepinsky R., Vedam K. Ferroelectric transition in Rubidium Bisulfate. Physical Review. **117** (6), 1502–1503 (1960).

[2] Ashmore J. P., Petch H. E. The structure of $RbHSO_4$ in paraelectric phase. Canadian Journal of Physics. **53** (24), 2694–2702 (1975).

[3] Iton K., Ohno H., Kuragaki S. Disordered structure of ferroelectric Rubidium Hydrogen Sulfate in the paraelectric phase. Journal of the Physical Society of Japan. **64**, 479–484 (1995).

[4] Zachek I. R., Shchur Ya., Levitskii R. R. Electromechanical and relaxation dielectric properties of $RbHSO_4$ crystal. Physica B: Condensed Matter. **478**, 113–121 (2015).

[5] Zachek I. R., Levitskii R. R., Shchur Ya., Bilenka O. B. Statistical theory of thermodynamic and dynamic properties of the $RbHSO_4$ ferroelectrics. Condensed Matter Physics. **18** (4), 43703 (2015).

[6] Zachek I. R., Levitsky R. R., Vdovych A. S. The influence of hydrostatic pressure p_h and shear stress σ_5 on the phase transitions and thermodynamics of the $RbHSO_4$ ferroelectrics. Journal of Physical Studies. **19** (3), 3703 (2015), (in Ukrainian).

[7] Zachek I. R., Karkuljevska M. S., Vdovych A. S., Levitsky R. R. Influence of External Pressures of Different Symmetry on the Phase Transitions and Thermodynamic of the $RbHSO_4$ Ferroelectrics. Physics and Chemistry of Solid State. **16** (2), 276–283 (2015), (in Ukrainian).

[8] Vdovych A. S., Levitskii R. R., Zachek I. R. Field and deformation effects in $RbHSO_4$ ferroelectric. Journal of Physical Studies. **24** (2), 2702 (2020).

[9] Kajikawa H., Ozaki T., Nakamura E. Dielectric critical phenomena in $RbHSO_4$. Journal of the Physical Society of Japan. **43**, 937–941 (1977).

[10] Gesi K., Ozawa K. Effect of Hydrostatic Pressure on Phase Transitions in Ferroelectric $RbHSO_4$ and $RbDSO_4$. Journal of the Physical Society of Japan. **38** (2), 459–462 (1975).

[11] Nakamura E., Kajikawa H. Dielectric properties of ferroelectric having small Curie–Weiss constant: rubidium hydrogen sulfate. Journal of the Physical Society of Japan. **44**, 519–524 (1978).

[12] Alexandrov K. S., Anistratov A. T., Blat D. X., Zherebtsova L. I., Zinenko V. I., Iskornev I. M., Melnikova S. V., Flerov I. N., Kirenski L. V. Properties on NH_4HSO_4 and $RbHSO_4$ single crystals near their Curie points. Ferroelectrics. **12**, 191–193 (1976).

[13] Aleksandrov K. S., Zaitseva M. P., Schmidt G., Shabanova L. A., Baige H. Elastic and nonlinear dielectric properties of the $RbHSO_4$ crystal in the vicinity of the ferroelectric phase transition. Crystallography. **26** (3), 610–613 (1981), (in Russian).

[14] Ozaki T. Dielectric Dispersion in Ferroelectric $RbHSO_4$. Journal of the Physical Society of Japan. **49** (1), 234–241 (1980).

[15] Grigas Y., Zachek I., Krasykov V., Kutnyi I., R. Levitskyi R., Paprotnyi V. Isotopic effect in $RbHSO_4$. Lit. Phys. Collection. **24** (6), 33–45 (1984), (in Russian).

[16] Ambrazyavichene V. S., Volkov A. A., Kozlov G. V., Krasykov V. S., Kryukova E. B. Acoustic and dielectric properties of the ferroelectric $RbHSO_4$ in the vicinity of the phase transition. Solid State Physics. **25** (6), 1605–1611 (1983), (in Russian).

[17] Paprotny W., Grigas J., Levitsky R. R., Kutny I. V., Krasikov V. S. Relaxational dielectric dynamics of $RbHSO_4$ crystals at microwaves. Ferroelectrics. **61** (1), 19–30 (1984).

Вплив одновісних тисків на динамічні діелектричні характеристики $RbHSO_4$

Левицький Р. Р.[1], Зачек І. Р.[2]

[1] *Інститут фізики конденсованих систем НАН України, вул. Свєнціцького, 1, 79011, Львів, Україна*
[2] *Національний університет "Львівська політехніка", вул. Бандери 12, 79013, Львів, Україна*

На основі модифікованої чотирипідграткової псевдоспінової моделі деформованого сегнетоелектрика $RbHSO_4$ в межах методу Глаубера в наближенні молекулярного поля розраховано динамічну діелектричну проникність механічно затиснутого кристала, а також досліджено вплив на неї одновісних тисків в широкому температурному і частотному діапазоні. Отримано задовільний кількісний опис відповідних експериментальних даних.

Ключові слова: *сегнетоелектрики, діелектрична динамічна проникність, вплив тиску.*